Nuclear Instruments and Methods in Physics Research B 267 (2009) 1899–1903

Contents lists available at ScienceDirect

Nuclear Instruments and Methods in Physics Research B

journal homepage: www.elsevier.com/locate/nimb

The (^{3}He, *tf*) as a surrogate reaction to determine (n, f) cross sections in the 10–20 MeV energy range

M.S. Basunia [a,*], R.M. Clark [a], B.L. Goldblum [b,e], L.A. Bernstein [b], L. Phair [a], J.T. Burke [b], C.W. Beausang [c], D.L. Bleuel [a], B. Darakchieva [c], F.S. Dietrich [b], M. Evtimova [c], P. Fallon [a], J. Gibelin [a], R. Hatarik [d], C.C. Jewett [b], S.R. Lesher [b,c], M.A. McMahan [a], E. Rodriguez-Vieitez [a], M. Wiedeking [a]

[a] *Lawrence Berkeley National Laboratory, Berkeley, California 94720, USA*
[b] *Lawrence Livermore National Laboratory, Livermore, California 94551, USA*
[c] *Department of Physics, University of Richmond, Richmond, Virginia 23173, USA*
[d] *Department of Physics and Astronomy, Rutgers University, Piscataway, New Jersey 08854, USA*
[e] *Department of Nuclear Engineering, University of California, Berkeley, California 94720, USA*

ARTICLE INFO

Article history:
Received 25 February 2009
Received in revised form 1 April 2009
Available online 23 April 2009

PACS:
24.85.+p
25.60.−t
25.60.Lg

Keywords:
Indirect method
Cross section
Surrogate Method
Charge-exchange reaction

ABSTRACT

The surrogate reaction ^{238}U(^{3}He, *tf*) is used to determine the ^{237}Np(n, f) cross section indirectly over an equivalent neutron energy range from 10 to 20 MeV. A self-supporting ~761 μg/cm^2 metallic ^{238}U foil was bombarded with a 42 MeV ^{3}He^{2+} beam from the 88-Inch Cyclotron at Lawrence Berkeley National Laboratory (LBNL). Outgoing charged particles and fission fragments were identified using the Silicon Telescope Array for Reaction Studies (STARS) consisted of two 140 μm and one 1000 μm Micron S2 type silicon detectors. The ^{237}Np(n, f) cross sections, determined indirectly, were compared with the ^{237}Np(n, f) cross section data from direct measurements, the Evaluated Nuclear Data File (ENDF/B-VII.0), and the Japanese Evaluated Nuclear Data Library (JENDL 3.3) and found to closely follow those datasets. Use of the (^{3}He, *tf*) reaction as a surrogate to extract (n, f) cross sections in the 10–20 MeV equivalent neutron energy range is found to be suitable.

Published by Elsevier B.V.

1. Introduction

Neutron-induced reaction cross section data for radioactive nuclei are important for various basic and applied sciences [1,2], however, target preparation for such studies is often complicated by material accessibility, availability, and radioactivity. The Surrogate Method provides access to such nuclear data indirectly [3]. In this method, the calculated compound-nucleus formation cross section of a neutron-induced reaction is combined with the experimentally measured decay probability of the compound nucleus, produced via a surrogate reaction, to the desired exit channel to obtain the neutron-induced cross section indirectly. A brief formalism of the Surrogate Method is presented in Section 2.

Earlier work on the indirect determination of neutron-induced fission cross section was reported in the 1970s [4–6]. In recent years, there has been a renewed effort both in the forefront of theory and experiment to utilize indirect methods more effectively to address nuclear data needs [7–12]. Younes and Britt [8] used earlier experimental data to demonstrate the possibilities and limitations of the Surrogate Method and to highlight the need for benchmarking studies. Employing the absolute Surrogate Method, Petit et al. [10] determined the ^{233}Pa(n, f) reaction cross sections in the 0.5–10 MeV equivalent neutron energy range using the ^{232}Th(^{3}He, p) surrogate reaction. In cases of contamination in the tagging channel from other nuclear reactions, rigorous data analysis is required and often the application of the absolute Surrogate Method is limited [10,11]. In the Surrogate Ratio Method (SRM), the determination of an unknown cross section relative to one that is well known removes the challenges posed by tagging channel contamination. The SRM is accomplished by performing the same surrogate reaction on two different targets and measuring a ratio of compound nuclear decay probabilities. Lyles et al. [11] and Burke et al. [12] successfully used (^{3}He, α) and (α, α′) reactions, as surrogate, to produce the desired compound nuclei and deduced the ^{236}U(n, f) and ^{237}U(n, f) cross sections, respectively, via the Surrogate Ratio Method. Recently, Nayak et al. [13] employed a hybrid surrogate ratio approach to determine the ^{233}Pa(n, f) reaction cross section from 11.5 to 16.5 MeV neutron energy using the ^{232}Th(^{6}Li, α) surrogate reaction.

* Corresponding author.
E-mail address: SBasunia@lbl.gov (M.S. Basunia).

0168-583X/$ - see front matter Published by Elsevier B.V.
doi:10.1016/j.nimb.2009.04.006

In this article, we report on the use of the ^{238}U(^{3}He, *tf*) reaction as a surrogate to determine the ^{237}Np(n, f) cross section over the neutron energy range of 10–20 MeV by the absolute Surrogate Method. The ^{237}Np(n, f) cross section is compared with the ^{237}Np(n, f) cross section data from direct measurements, the Evaluated Nuclear Data File (ENDF/B-VII.0), and the Japanese Evaluated Nuclear Data Library (JENDL 3.3) to study the (^{3}He, *tf*) reaction as a surrogate in the 10–20 MeV energy range.

2. The Surrogate Method

In the Hauser–Feshbach formulation [14], the cross-section, $\sigma_{\alpha\chi}$, for forming a compound nucleus (CN) via entrance channel α and its subsequent decay via exit channel χ (^{237}Np + n and fission, respectively, here) can be expressed as:

$$\sigma_{\alpha\chi} = \sum_{J,\pi} \sigma_{\alpha}^{CN}(E^*, J, \pi) G_{\chi}^{CN}(E^*, J, \pi), \quad (1)$$

where E^*, J, and π are the excitation energy, total angular momentum, and parity of the CN, σ_{α}^{CN} is the compound nuclear formation cross section via entrance channel α and G_{χ}^{CN} is the probability of the CN decay through exit channel χ. In the case for neutrons incident on ^{237}Np, the formation cross section σ_{α}^{CN} can be calculated within 6% uncertainty using an optical model formalism (as discussed in Section 3.2.), whereas the decay probabilities, G_{χ}^{CN}, are difficult to ascertain via theoretical models. In the Surrogate Method, the CN of the desired reaction is produced via a different combination of target and projectile. An expression for the probability, $P_{\delta\chi}(E^*)$, for formation of the CN via the surrogate entrance channel δ (δ, in this work, ^{238}U(^{3}He, t)), and its subsequent decay via exit channel χ (here, fission) can be written as:

$$P_{\delta\chi}(E^*) = \sum_{J,\pi} F_{\delta}^{CN}(E^*, J, \pi) G_{\chi}^{CN}(E^*, J, \pi), \quad (2)$$

where F_{δ}^{CN} represents the probability of populating states in the CN via the surrogate reaction with a given excitation energy, E^*, total angular momentum J, and parity π. The exit channel decay probabilities, G_{χ}^{CN}, are the same as those that appear in Eq. (1).

In the Weisskopf–Ewing limit [15] of the Hauser–Feshbach theory, the decay probabilities are independent of the total angular momentum and parity of the populated states and can be taken out of the summation signs in Eqs. (1) and (2). The resultant equation for the desired reaction cross section in terms of the experimentally observable surrogate reaction probability becomes:

$$\sigma_{\alpha\chi}(E^*) = \sigma_{\alpha}^{CN}(E^*) P_{\delta\chi}(E^*). \quad (3)$$

It may be noted here that $\sum_{J,\pi} F_{\delta}^{CN}(E^*, J, \pi) = 1$ in the Surrogate Method, since the probability of decay of the desired CN, produced by the surrogate reaction, is always measured in coincidence with an ejected particle that ensures the formation of the desired CN. In this work, the probability of fission of the CN ^{238}Np*, produced by the surrogate reaction ^{238}U(^{3}He,t)^{238}Np, is measured in coincidence with tritons.

Finally, the experimentally measured fission probability, $P_{\delta\chi}(E^*)$, of the ^{238}Np* is multiplied by the calculated CN formation cross section, σ_{α}^{CN}, for neutrons incident on ^{237}Np to deduce the desired ^{237}Np(n,f) cross section.

3. Experiment

3.1. Target, the detector assembly, and irradiation

In the experiment, a self-supporting 99.99% pure metallic ^{238}U foil of thickness 4709 ± 235 Å (761 ± 38 μg/cm^2) was bombarded with a 42 MeV ^{3}He^{2+} beam from the 88-Inch Cyclotron at Lawrence Berkeley National Laboratory with a beam current of approximately 2–3 pnA over a period of 8 days. The beam spot on the target was approximately 3 mm in diameter. Outgoing charged particles were identified using one 140 μm and one 1000 μm Micron S2 type silicon detectors as a $\Delta E + E$ particle telescope covering an angular range of 36°–66° with respect to the beam axis. Another 140 μm silicon detector was used to detect fission fragments during the experiment over the backward angular range of 106°–131°. The schematic diagram of the target and the detector locations for the experimental setup is shown in Fig. 1. The target was placed 15 mm upstream of the particle telescope in the incoming beam direction and the fission detector was placed 10 mm upstream from the target. Each of the double-sided S2 type silicon detectors has 22 mm active inner diameter and 70 mm active outer diameter with 48 rings on one side and 16 sectors on the opposite side. In this experiment, pairs of adjacent rings and sectors were bussed together to form 24 rings and 8 sectors. A 4.44 mg/cm^2 thick aluminum foil was placed between the target and the particle telescope to stop the fission fragments and thereby protect the ΔE detector from damage. Detailed description of the experimental setup and electronics of the detection system is provided in [11]. All silicon detectors were energy calibrated using ^{241}Am and ^{226}Ra α-lines.

3.2. Data analysis

The ΔE vs. E plots were used to identify different particles (p, d, t, ^{3}He and ^{4}He), as shown in Fig. 2 for a single ring of the ΔE detector. Gates on the triton particles were set for each ring of the Si detector separately. Fully stopped particles in the particle telescope form a banana shape in the ΔE vs. E plots. Particles that are not stopped in the E detector ("punch-through" particles) form a reverse tail at the lower end of the banana shape as shown in Fig. 2. In all triton gates, the punch-through particles were rejected due to incomplete charge deposition. The initial triton energy is reconstructed on an event-by-event basis for energy losses in the target, aluminum δ-shield, and gold layers of the silicon detectors. Using a Time-to-Amplitude Converter (TAC) gate, off-prompt triton–fission coincident events were distinguished from the prompt events and used in background correction of the prompt triton–fission coincidences.

Singles triton spectra and coincident fission spectra for all rings of the particle telescope and fission detector were integrated. The integrated triton spectrum and background-corrected fission spectrum are presented in Fig. 3 as a function of ^{238}Np* excitation energy. The excitation energy of the ^{238}Np* in the center-of-mass system is obtained using the measured triton energy, a Q-value of −0.166 MeV for the ^{238}U(^{3}He,t)^{238}Np reaction and the beam en-

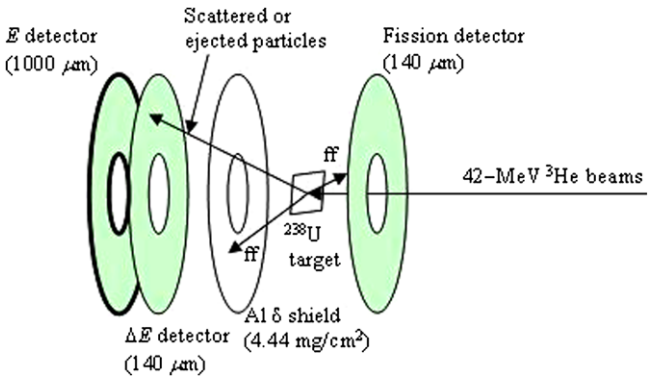

Fig. 1. Experimental setup of ^{238}U target, silicon telescope ($\Delta E + E$), Al shield, and fission detector. Arbitrary directions for the scattered/ejected particle and fission fragment (ff) along with the incoming beam on the ^{238}U target are shown.

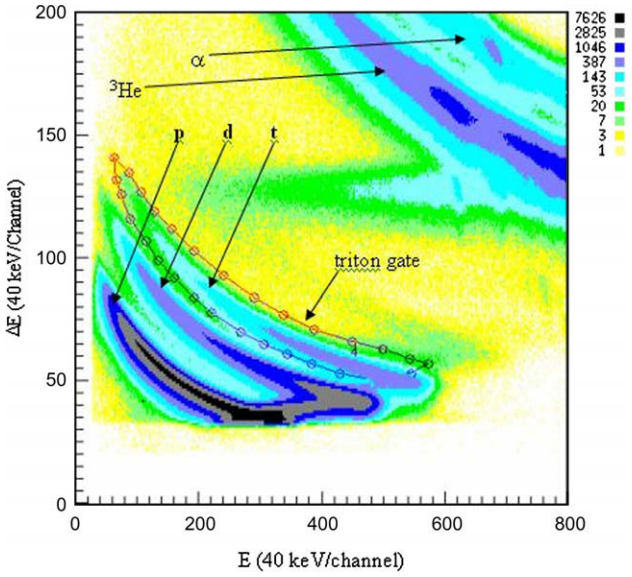

Fig. 2. ΔE vs. E plot for a single ring at 49° with respect to the beam axis shows different ejected particles from the interaction of 42 MeV ^{3}He beams with the ^{238}U target. Protons (p), deuterons (d), and tritons (t) are located in the lower left side in the plot and part of the ^{3}He and α particles are visible in the upper right corner in the plot. A typical triton gate is shown.

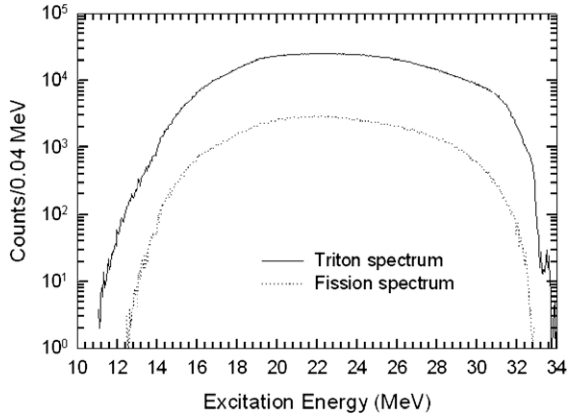

Fig. 3. Integrated singles triton spectrum and background-corrected fission spectrum of the particle telescope and fission detector.

ergy. The reported range of 10–20 MeV equivalent neutron energy of this work corresponds to approximately 15.5–25.5-MeV ^{238}Np* excitation energy. High (low) ^{238}Np* excitation energy corresponds to low (high) triton energy. Cross section data for equivalent neutron energies corresponding to less than approximately 15.5 MeV of excitation energy were discarded due to possible partial energy deposition ("punch-through") of the tritons in the particle telescope. Above 25.5 MeV excitation energy (low triton energy), there may be significant contribution of additional tritons from the nuclear interaction of the beam with ^{16}O oxidative contaminants in the target material [^{16}O(^{3}He,t)^{16}F, $E_{\text{threshold}}$ = 18.3 MeV] and from the ^{3}He breakup-transfer mechanism, prominent at forward angles [16]. Such additional tritons lower the deduced fission probability and thereby reduce the extracted cross section. This imposes an upper limit on the equivalent neutron energy extracted from the absolute Surrogate Method. Since the (^{3}He,t) reaction has a higher energy threshold for common contaminants, i.e. oxygen and carbon isotopes, than other surrogate reactions, like (α,α′) or (^{3}He,α), the (^{3}He,t) charge exchange reaction was useful for suppressing contaminant events over a wide equivalent neutron energy range.

A total of approximately 10^7 tritons and their coincident fission events were analyzed in this work. Histograms of 120 keV energy bins of the triton and coincident fission spectra were used to deduce the fission probability of the compound nucleus ^{238}Np* using the following equation:

$$P_{\delta\chi}(E^*) = P_f(E^*) = \frac{N_{cf}}{N_t}\frac{1}{\varepsilon(E^*)}, \tag{4}$$

where N_t is the number of detected tritons, N_{cf} is the number of recorded fission events in coincidence with emitted tritons and $\varepsilon(E^*)$ is the efficiency of the fission detector. In this work, the efficiency of the fission detector was extracted by normalizing the fission probability with the known fission probability of ^{238}Np* at an excitation energy equivalent to 10 MeV incident neutron energy [17]. This neutron energy is chosen arbitrarily. The extracted fission detector efficiency was used to deduce the fission probability as a function of ^{238}Np* excitation energy and presented in Fig. 4.

The compound-nucleus formation cross section for the ^{237}Np + n was calculated for different incident neutron energies using the Flap2.2 optical-model potential [18]. The Flap2.2 optical potential is a coupled-channel potential that was determined by fitting a selection of neutron data in the actinides, including the s- and p-wave strength functions and potential scattering radius for ^{232}Th and ^{238}U, as well as total cross sections in the 1–100 MeV range for these nuclei. The parameterization included isovector terms in both real and imaginary central potentials, with strength 1/2 that of the corresponding isoscalar terms. For even–even nuclei, the 3 lowest states of the ground-state band are coupled, while for odd-mass nuclei, the lowest five states are included. For the calculations of ^{237}Np + n, the deformation parameters for the central potential were chosen as $\beta_2 = 0.214$ and $\beta_4 = 0.074$; these were taken from [19]. The resulting compound-nucleus formation cross section (the full non-elastic cross section minus the sum of the calculated cross sections for direct inelastic scattering) is shown in Fig. 5. Based on comparison with measurements of this quantity in ^{238}U (see [20,21]), we estimate the uncertainty in the calculated cross sections as approximately ±6% below 10 MeV and ±3% in the range 10–30 MeV.

Finally, at the incident neutron energy E_n leading to same excitation energy E^*, the ^{237}Np(n,f) cross section was deduced using the form of Eqs. (3) and (4) as:

$$\sigma_{nf}(E_n) \approx P_f\left(E^* = S_n + \frac{A}{A+1}E_n\right)\sigma_n^{CN}(E_n), \tag{5}$$

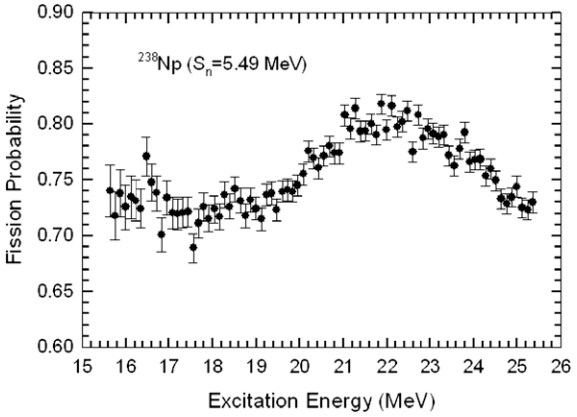

Fig. 4. Measured fission probabilities of the ^{238}Np* produced from the ^{238}U(^{3}He, tf) reaction. Error bars show the statistical uncertainty only. Threshold of ^{238}Np* third chance fission is 18.2 MeV excitation energy.

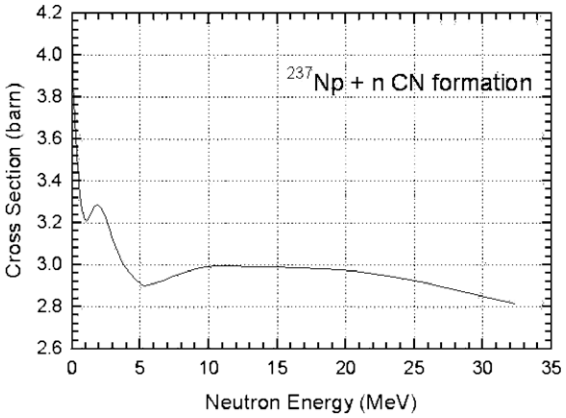

Fig. 5. Calculated ^{237}U + n compound-nucleus formation cross section.

where S_n is the neutron separation energy in the residual CN and the term $\frac{A}{A+1}E_n$ is the channel energy for the reaction when the target (mass A) is at rest [22].

3.3. Sources of uncertainty

The sources of uncertainty for the neutron energy were the energy straggle of the triton, angular resolution, beam energy resolution and detector resolution. The estimated uncertainties are presented in Table 1. The energy straggle arises from the interaction of tritons with the aluminum δ-shield and gold layers of the silicon detector. In this experiment, the angular resolution ranged between 0.7° and 2.3°. The angular resolution translates into an uncertainty of the recoil angle of the product nucleus. The cyclotron beam energy resolution of 60–80 keV is obtained from the beam width, measured by placing a calibrated silicon detector directly in an α beam from the 88-Inch. cyclotron [12]. Including an estimated uncertainty of the detector energy calibration, a total uncertainty of 0.2 MeV is attributed over the neutron energy range from 10 to 20 MeV.

The uncertainty in the cross section arises from the counting statistics of the fission events, uncertainty in the fission detector efficiency and uncertainty of the calculated CN formation cross section. The statistical uncertainty for the fission events in each 120-keV energy bin was between 1% and 3%. The uncertainty of the fission detector efficiency estimated to be 10%. An uncertainty of 3% for the CN formation cross section calculation is estimated for the 10 to 20 MeV neutron energy range.

Table 1
Source and uncertainty for the neutron energy and reported cross section.

Neutron energy		Cross section	
Source	ΔE (keV)	Source	Magnitude (%)
Energy straggle of triton (δ-shield and gold layer of Si detector)	10–23	Counting statistics	1–3
Recoil angle of triton	6–26	^{237}Np + n CN formation (calculation)	3
Detector energy resolution	38–55		
Beam energy	60–80	Fission detector efficiency	10

4. Results

The extracted ^{237}Np(n,f) reaction cross section of this work, determined using the surrogate reaction ^{238}U(^{3}He,tf), is presented in Fig. 6(a) along with the direct measurement from [23] and adopted cross section data from the Evaluated Nuclear Data File (ENDF/B-VII.0) and the Japan Evaluated Nuclear Data Library (JENDL 3.3). It can be seen from Fig. 6(a) that the ^{237}Np(n,f) cross section data of this work closely follow the trend of the directly measured data [23] and the ENDF/B-VII.0 data through the onset of third chance fission (at approximately 12.5 MeV neutron energy) of ^{238}Np* and onward. The cross sections of this work are approximately 5% higher when compared to the ENDF/B-VII.0 data. The trend of the JENDL data is slightly lower than our data and the discrepancy is slightly larger than that with the ENDF dataset. Recently, Tovesson and Hill [24] published a cross section ratio for the ^{237}Np(n,f) to the ^{235}U(n,f) nuclear reaction. A ratio of the determined cross section for the ^{237}Np(n,f) from this work to the

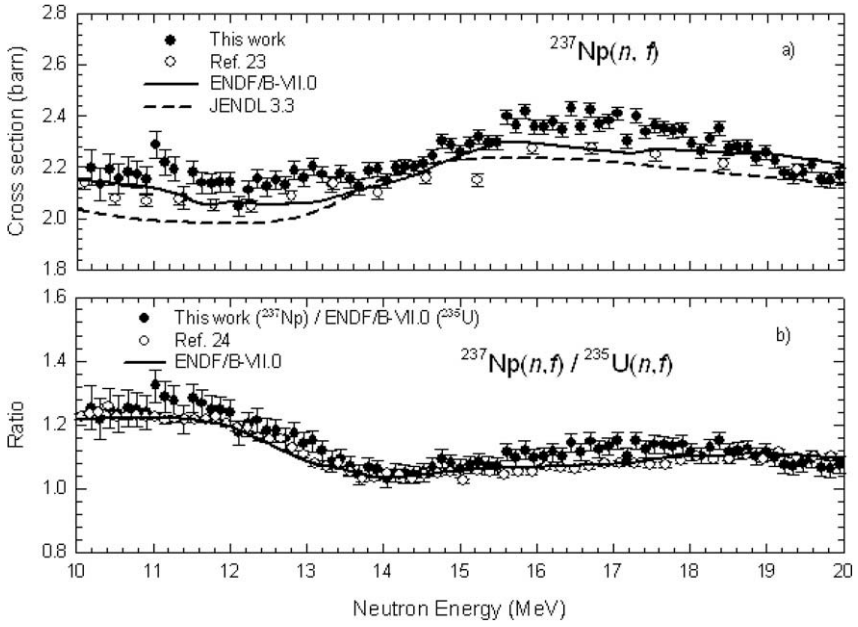

Fig. 6. (a) Cross sections for the ^{237}Np(n, f) reaction and (b) ratio for the ^{237}Np(n, f) to ^{235}U(n, f) cross sections of this work along with measured and evaluated data. The ratio for this work in (b) was generated using the ^{235}U(n, f) data from ENDF/B-VII.0. Error bars show only the statistical uncertainty.

^{235}U(n,f) cross section, obtained from the ENDF/B-VII.0 database, is presented in Fig. 6(b) along with the ratio data of [24] and a generated ratio from the ENDF/B-VII.0 database. Again it can be seen that the deduced ratio of this work follows the same trend with the others, with slight variation over the reported neutron energy range. The agreement of the results with the directly measured data shows that the contamination in the triton exit channel from other reactions or from ^{3}He breakup-transfer mechanism was insignificant in the 10–20 MeV equivalent neutron energy range.

5. Conclusion

The surrogate reaction ^{238}U(^{3}He,tf) was used to extract the ^{237}Np(n,f) cross section in the 10–20 MeV equivalent neutron energy range. The agreement of the indirectly determined ^{237}Np(n,f) cross section of this work with the ^{237}Np(n,f) cross section from direct measurements, the Evaluated Nuclear Data File (ENDF/B-VII.0), and the Japanese Evaluated Nuclear Data Library (JENDL 3.3) is found to be very good. The use of (^{3}He,tf) reaction as a surrogate to extract (n,f) cross sections in the 10–20 MeV equivalent neutron energy was effective and minimal efforts were needed to address the contamination concerns to measure the fission probability of the desired compound nucleus ^{238}Np*. This work reported the first study on the effectiveness of the (^{3}He,tf) reaction as a surrogate for extracting (n,f) cross section in the 10–20 MeV energy range.

Acknowledgements

We wish to thank the 88-Inch Cyclotron operation team at LBNL for their help in performing the irradiations for this experiment. We are grateful to R. Foreman for making the ^{238}U target for this experiment. This work was performed under the auspices of the US Department of Energy by the University of California, Lawrence Berkeley National Laboratory under contract No. DE-AC02-05CH11231 and an LDRD project, Lawrence Livermore National Laboratory under Contract Nos. W-7405-Eng-48 and DE-AC52-07NA27344, and the University of Richmond contract Nos. DE-FG-05NA25929 and DE-FG02-05ER41379.

References

[1] S. Kubono, Nucl. Phys. A 693 (2001) 221.
[2] G. Aliberti, G. Palmiotti, M. Salvatores, T.K. Kim, T.A. Taiwo, M. Anitescu, I. Kodeli, E. Sartori, J.C. Bosq, J. Tommasi, Ann. Nucl. Energy 33 (2006) 700.
[3] J. Escher, L. Ahle, L. Bernstein, J. Burke, J.A. Church, F. Dietrich, C. Forssén, V. Gueorguiev, R. Hoffman, J. Phys. G: Nucl. Part. Phys. 31 (2005) S1687.
[4] H.C. Britt, J.B. Wilhelmy, Nucl. Sci. Eng. 72 (1979) 222.
[5] A. Gavron, H.C. Britt, P.D. Goldstone, R. Schoenmackers, J. Weber, J.B. Wilhelmy, Phys. Rev. C 15 (1977) 2238.
[6] J.D. Cramer, H.C. Britt, Nucl. Sci. Eng. 41 (1970) 177.
[7] J.E. Escher, F.S. Dietrich, C. Forssén, Nucl. Instr. and Meth. B 261 (2007) 1075.
[8] W. Younes, H.C. Britt, Phys. Rev. C 67 (2003) 024610.
[9] J.E. Escher, F.S. Dietrich, Phys. Rev. C 74 (2006) 054601.
[10] M. Petit, M. Aiche, G. Barreau, S. Boyer, N. Carjan, S. Czajkowski, D. Dassié, C. Grosjean, A. Guiral, B. Haas, D. Karamanis, S. Misicu, C. Rizea, F. Saintamon, S. Andriamonje, E. Bouchez, F. Gunsing, A. Hurstel, Y. Lecoz, R. Lucas, Ch. Theisen, A. Billebaud, L. Perrot, E. Bauge, Nucl. Phys. A 735 (2004) 345.
[11] B.F. Lyles, L.A. Bernstein, J.T. Burke, F.S. Dietrich, J. Escher, I. Thompson, D.L. Bleuel, R.M. Clark, P. Fallon, J. Gibelin, A.O. Macchiavelli, M.A. McMahan, L. Phair, E. Rodriguez-Vieitez, M. Wiedeking, C.W. Beausang, S.R. Lesher, B. Darakchieva, M. Evtimova, Phys. Rev. C 76 (2007) 014606.
[12] J.T. Burke, L.A. Bernstein, J. Escher, L. Ahle, J.A. Church, F.S. Dietrich, K.J. Moody, E.B. Norman, L. Phair, P. Fallon, R.M. Clark, M.A. Deleplanque, M. Descovich, M. Cromaz, I.Y. Lee, A.O. Macchiavelli, M.A. McMahan, L.G. Moretto, E. Rodriguez-Vieitez, F.S. Stephens, H. Ai, C. Plettner, C. Beausang, B. Crider, Phys. Rev. C 73 (2006) 054604.
[13] B.K. Nayak, A. Saxena, D.C. Biswas, E.T. Mirgule, B.V. John, S. Santra, R.P. Vind, R.K. Choudhury, S. Ganesan, Phys. Rev. C 78 (2008) 061602 (R).
[14] W. Hauser, H. Feshbach, Phys. Rev. 87 (1952) 366.
[15] V.F. Weisskopf, D.H. Ewing, Phys. Rev. 57 (1940) 472.
[16] E.H.L. Aarts, R.K. Bhowmik, R.J. De Meijer, S.Y. Van Der Werf, Phys. Lett. B 102 (1981) 307.
[17] V.M. Pankratov, J. Nucl. Energy 18 (1964) 215.
[18] J.E. Escher, F.S. Dietrich, Tech. Rep. UCRL-TR-212509, Lawrence Livermore National Laboratory, Livermore, CA, 2005.
[19] P.G. Young, Report LA-UR-94-3104, Los Alamos National Laboratory, Los Alamos, NM, 1994, <http://library.lanl.gov/cgi-bin/getfile?00411586.pdf>.
[20] F.S. Dietrich, J.D. Anderson, R.W. Bauer, S.M. Grimes, in: R.C. Haight et al. (Eds.), Proceedings of International Conference on Nuclear Data for Science and Technology, Santa Fe, NM, 26 September–1 October, 2004, AIP Conference Proceedings No. 769, Melville, New York, 2005, p. 300.
[21] M.H. MacGregor, R. Booth, W.P. Ball, Phys. Rev. 130 (1963) 1471.
[22] P.E. Hodgson, E. Gadioli, E. Gadioli Erba, Introductory Nuclear Physics, Clarendon, Oxford, 1997. p. 226.
[23] O. Shcherbakov, A. Donets, A. Evdokimov, A. Fomichev, T. Fukahori, A. Hasegawa, A. Laptev, V. Maslov, G. Petrov, S. Soloviev, Y. Tuboltsev, A. Vorobyev, J. Nucl. Sci. Tech. (Suppl. 2) (2002) 230.
[24] F. Tovesson, T.S. Hill, Phys. Rev. C 75 (2007) 034610.